

Article

Improved Rotor Braking Protection Circuit and Self-Adaptive Control for DFIG during Grid Fault

Jiming Chen ^{*}, Yuanhao Wang, Mingxiao Zhu , Qianyu Yu and Jiakai Li 

College of Information and Control Engineering, China University of Petroleum (East China), Qingdao 266580, China; yhwangupc@163.com (Y.W.); zhumx@upc.edu.cn (M.Z.); upcyqy@126.com (Q.Y.); jiakai@s.upc.edu.cn (J.L.)

^{*} Correspondence: jimingchen@upc.edu.cn

Received: 24 April 2019; Accepted: 22 May 2019; Published: 24 May 2019



Abstract: This paper introduces an improved rotor braking protection circuit configuration and the corresponding self-adaptive control strategy to enhance the low voltage ride-through (LVRT) capability of the doubly-fed induction generator (DFIG). The proposed protection circuit consists of a crowbar circuit and a series rotor braking resistor array, which guarantees the safe operation of wind generators under the LVRT. Moreover, to adapt the proposed protection and further enhance the performance of the improved configuration, a corresponding self-adaptive control strategy is presented, which regulates the rotor braking resistor and protection exiting time automatically through calculating the rotor current in the fault period. The LVRT capability and transient performance of the DFIG by using the proposed method is tested with simulation. Compared with the conventional crowbar protection or the fixed rotor braking protection, the proposed protection and the control strategy present several advantages, such as retaining the control of the rotor side converter, avoiding repeated operation of the protection and accelerating the damping of stator flux linkage during a grid fault.

Keywords: DFIG; rotor braking circuit; crowbar; low voltage ride-through; self-adaptive control

1. Introduction

Since the limitation of the fossil fuel becomes a public concern, renewable energy is getting more and more attention in recent years. As one of the most dominant renewable sources, wind energy is extensively exploited in power system. In the meantime, the power grid is faced with a series of challenges brought by wind turbines. Especially, the introduced low voltage ride-through (LVRT) issue is a major cause of generator-shedding and power system stability. In order to support the voltage during grid fault, numerous power utilities put forward strict grid codes which require wind turbines not only to remain connected with the power grid but also inject reactive current into the grid [1].

The doubly-fed induction generator (DFIG) is widely used in wind power generation systems due to its several advantages, such as variable speed operation. However, when a grid fault occurs, the DFIG is faced with the danger of overcurrent on both stator and rotor sides [2] for its sensitivity to grid fault. Insulated gate bipolar transistors (IGBTs) of the rotor side converter (RSC) may be damaged by the impact current. In addition to overcurrent, the DC-link overvoltage also threatens the security of the DFIG [3].

Several approaches have been presented to protect the DFIG and enhance its LVRT capability. A widely applied method is crowbar protection in rotor circuit [4], which has a simple structure and restrains the overcurrent effectively. However, the RSC is blocked when crowbar is active. In this circumstance, the DFIG operates as an induction machine and consumes reactive power from the power grid [5] which deepens the voltage sag. A capacitor in series with crowbar circuit is proposed to

eliminate the ripples in the rotor circuit and DC-link in [6]. This reduces crowbar operating time but cannot avoid blocking the RSC. Employing a series dynamic braking resistor (SDBR) in the stator or rotor circuit, as in [7–9], improves transient responses under a grid fault and avoids blocking the RSC. In addition, stator SDBR restrains the rotor current and DC-link voltage significantly and promotes the terminal voltage [8]. However, the stator SDBR absorbs active power and rotor SDBR may cause a high rotor voltage [10]. In [11], a dynamic voltage restorer (DVR) is adopted, which compensates the grid voltage and allows the DFIG operates uninterruptedly. Simultaneously, the DVR increases the cost and complexity of the DFIG. Combining with crowbar circuit, a R-L impedance circuit in series with rotor circuit was introduced in [12,13], which maintains the RSC partial connection to the rotor. In order to retain the control of the RSC and enhance the transient performance during the fault grid, the protection circuit is still expected to be improved. The fault current limiter is adopted in [14–17] to limit the fault current and enhance the LVRT ability. In [18–20], the control strategies of the RSC are proposed, which controls the RSC generating the rotor current for demagnetizing.

This paper proposes an improved configuration to enhance the LVRT capability of the DFIG and avoid blocking the RSC. A corresponding control strategy is also provided. The proposed configuration is composed of a crowbar and a rotor braking resistor array in series with the rotor circuit between the crowbar and the RSC. The series rotor braking resistor array restrains the RSC current below the maximum current of the IGBTs. Using the crowbar circuit as a part of the protection, the proposed method cannot avoid absorbing reactive power due to the crowbar current, which would reduce the effect of reactive power control. It can be solved partly through an appropriate selection of parameters. The rotor current is calculated and the parameter selection principle is given, by which the rotor current and RSC current remains at an appropriate value.

To improve the transient performance, a corresponding self-adaptive control is employed, which regulates the rotor braking resistance and protection exiting time automatically according to the fault situation and calculation results in the LVRT process. Finally, a 1.5 MW DFIG simulation model is developed to validate the effectiveness of the proposed configuration and control strategy. Compared with the conventional crowbar protection, the fluctuation of the rotor current and the electromagnetic torque under the proposed protection is slightly larger due to the operation of the RSC and the variation of the resistor array. However, the RSC is blocked in the conventional crowbar protection, which brings trouble to the DFIG. Employing the proposed configuration, the control of the RSC is retained. As a result, the reactive power control of the DFIG can be carried out and the grid voltage is supported during the fault period. Additionally, the comparisons of the simulation results also show that the self-adaptive control avoids the repeated operation of the protection and accelerates the damping of the stator flux linkage.

2. Mathematical Model of the DFIG

The structure of wind power system driven by the DFIG is described in Figure 1, which is composed of a wind turbine, gear box, DFIG, power electronic converter, and control system [21].

The stator of the DFIG is connected with the power grid directly and the rotor is connected with the power grid through a power electronic converter which consists of the RSC and the grid side converter (GSC) [22]. When the DFIG is operating, both stator and power electronic converter can exchange power with the power grid. The power flow of the power electronic converter tends to be static when the generator is operating synchronously. Through the control system, the amplitude and frequency of rotor voltage is controlled and variable speed operation is realized.

Using the Park's model, voltage equations can be described as in a d-q synchronous reference frame:

$$\begin{cases} u_{sd} = R_s i_{sd} + p\psi_{sd} - \omega_1 \psi_{sq} \\ u_{sq} = R_s i_{sq} + p\psi_{sq} + \omega_1 \psi_{sd} \\ u_{rd} = R_r i_{rd} + p\psi_{rd} - s\omega_1 \psi_{rq} \\ u_{rq} = R_r i_{rq} + p\psi_{rq} + s\omega_1 \psi_{rd} \end{cases} \quad (1)$$

where u_s and u_r are the stator and rotor voltage vector, respectively. i_s and i_r are the stator and rotor current vector, respectively. ω_1 is the synchronous angular speed and s is the slip ratio.

Flux linkage equations can be described as well in Equation (2)

$$\begin{cases} \psi_{sd} = L_s i_{sd} + L_m i_{rd} \\ \psi_{sq} = L_s i_{sq} + L_m i_{rq} \\ \psi_{rd} = L_r i_{rd} + L_m i_{sd} \\ \psi_{rq} = L_r i_{rq} + L_m i_{sq} \end{cases} \quad (2)$$

where ψ_s and ψ_r are the stator and rotor flux linkages, respectively; L_m is the magnetizing inductance, L_s is the total inductance in stator circuit, and L_r is the total inductance in rotor circuits.

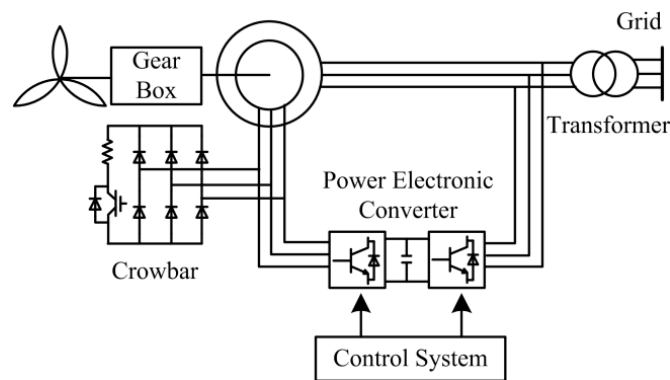


Figure 1. Structure of wind turbine driven by a DFIG.

Employing grid voltage orientation, the active and reactive power produced by stator is written as follows:

$$\begin{cases} P_s = -\frac{3}{2}(u_{sd}i_{sd} + u_{sq}i_{sq}) \approx \frac{3}{2}\frac{L_m}{L_s}u_s i_{rd} \\ Q_s = -\frac{3}{2}(u_{sq}i_{sd} - u_{sd}i_{sq}) \approx -\frac{3u_s}{2\omega_1 L_s}(u_s + \omega_1 L_m i_{rq}) \end{cases} \quad (3)$$

From Equation (3), it can be concluded that the active power and reactive power of stator are controlled by the rotor current. A similar conclusion can also be obtained in the GSC:

$$\begin{cases} P_g = \frac{3}{2}u_{gd}i_{gd} \\ Q_g = -\frac{3}{2}u_{gd}i_{gq} \end{cases} \quad (4)$$

Combining Equation (1) with (2), the rotor voltage can be expressed as follows:

$$u_r = e_r + R_r i_r + (L_r - \frac{L_m^2}{L_s}) \frac{di_r}{dt} + j\omega_p (L_r - \frac{L_m^2}{L_s}) i_r \quad (5)$$

where ω_p is slip angular speed; e_r is the rotor induced voltage that affected by stator flux linkage through:

$$e_r = \frac{L_m}{L_s} \frac{d\psi_s}{dt} + j\omega_p \frac{L_m}{L_s} \psi_s \quad (6)$$

According to Equation (5), the rotor equivalent circuit of the DFIG is presented in Figure 2, where $\sigma = 1 - L_m^2/L_s L_r$.

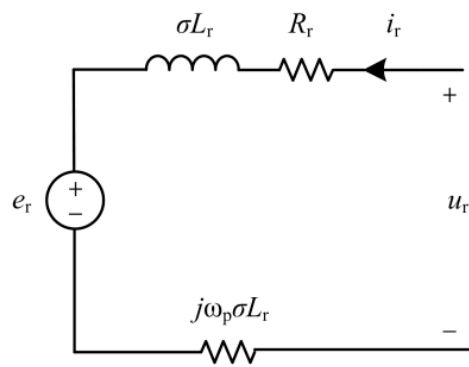


Figure 2. Rotor equivalent circuit of the DFIG.

During the fault period, the stator flux linkage used the synchronous reference frame is:

$$\psi_s = \frac{(1 - K_d)U_{s0}}{j\omega_1} + \frac{K_d U_{s0}}{j\omega_1} e^{-j\omega_1 t} e^{-t/T_s} \quad (7)$$

where U_{s0} is steady-state voltage and T_s is stator time constant. K_d is the depth of voltage sag and it can be expressed as:

$$K_d = 1 - \frac{U_s}{U_{s0}} \quad (8)$$

where U_s is the fault voltage. Hence, Equation (6) becomes:

$$e_r = e_{\text{rof}} + e_{\text{ron}} \quad (9)$$

$$e_{\text{rof}} = j\omega_p \frac{L_m (1 - K_d) U_{s0}}{L_s j\omega_1} \quad (10)$$

$$e_{\text{ron}} = \frac{L_m K_d U_{s0}}{L_s j\omega_1} (\lambda + j\omega_p) e^{\lambda t} \quad (11)$$

where $\lambda = -j\omega_s - 1/T_s$. The e_{rof} is the steady-state component of e_r and the e_{ron} is the transient component that decreases exponentially.

As it is shown in Equations (7)–(11), when a grid fault occurs, the stator flux linkage increases and then the rotor induced voltage increases. However, the RSC cannot provide a corresponding exciting voltage, thus, an overcurrent is produced in rotor circuit. The IGBTs of the RSC may be damaged if the overcurrent exceeds the safety threshold and, hence, protection is necessary.

3. Improved Rotor Braking Protection

This section introduces an improved configuration of rotor braking protection firstly. In addition, to prove the effectiveness of the proposed circuit, the equivalent circuit and related theoretical calculations are given. The parameter selection principle is also presented in the last section.

3.1. Proposed Configuration

As what is analyzed in Section 2, protection should be applied during the fault time. The crowbar circuit is a prevalent method for DFIG protection. When the crowbar is operating, the crowbar resistor is connected with the rotor circuit and rotor current is restrained. However, to protect the RSC, the RSC is blocked in the crowbar operating period and the DFIG operates as an induction machine, which absorbs reactive power from the grid and deepens the voltage sag.

To avoid blocking the RSC and enhance the LVRT capability of the DFIG, an improved configuration of the protection circuit is proposed in Figure 3. It is composed of two sections: (1) a crowbar circuit, and (2) a series rotor braking circuit.

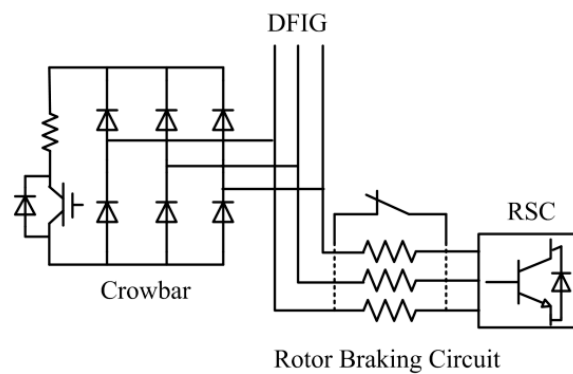


Figure 3. Configuration of the proposed protection.

A rotor braking circuit in series with the rotor circuit between the RSC and crowbar circuit is presented. The series rotor braking circuit is shortened by a switch normally and the switch would break during the grid fault period. When the rotor braking circuit operates solely, the RSC current would be restrained below the maximum current of the RSC. As a result, the RSC avoids being blocked and its control is retained.

As it is explained above, that the variation of e_r causes rotor overcurrent, the damping of the rotor current is closely related to the structure of the rotor circuit. When the rotor braking circuit operates solely, the rotor current can be written as follow:

$$u_r = e_r + (R_r + R_{ser})i_r + \sigma L_r \frac{di_r}{dt} + j\omega_p \sigma L_r i_r \tag{12}$$

where R_{ser} is the rotor braking resistance. Solving the differential equation in Equation (12), it can be found that the rotor current decreases exponentially with the stator time constant T_s and rotor time constant T_r . The rotor time constant is:

$$T_r = \frac{\sigma L_r}{R_r + R_{ser}} \tag{13}$$

The less the rotor time constant is, the faster the rotor transient current dampens. With the operation of the series resistor, the rotor resistor increases equivalently and, therefore, the rotor time constant decreases, which is beneficial for the protection.

According to Equation (1) and Equation (2), the stator equivalent circuit of the DFIG is shown in Figure 4.

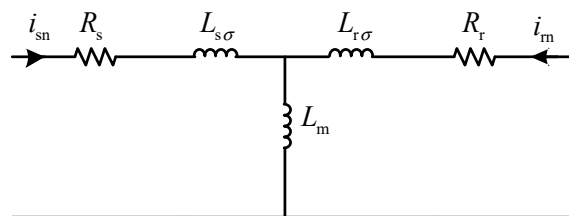


Figure 4. Equivalent circuit of the DFIG.

The rotor resistor can be ignored and the rotor current is written as:

$$i_r = -\frac{L_m}{L_r} i_s \tag{14}$$

According to Equations (2) and (14), the stator flux linkage becomes:

$$\psi_s = (L_s - \frac{L_m^2}{L_r})i_s = L'_s i_s \tag{15}$$

where L'_s is the equivalent stator inductor. As a result, the stator time constant can be expressed as:

$$T_s = \frac{L'_s}{R_s} = \frac{L_s}{R_s} - \frac{L_m^2}{R_s L_r} \tag{16}$$

When the rotor braking circuit is operating, the resistor of the rotor circuit cannot be ignored due to the high value of the rotor braking resistor. Equations (14)–(16) are changed as follows:

$$i_r = -\frac{j\omega_p L_m}{R_r + R_{ser} + j\omega_p L_r} i_s \tag{17}$$

$$\psi_s = (L_s - \frac{j\omega_p L_m^2}{R_r + R_{ser} + j\omega_p L_r})i_s = L''_s i_s \tag{18}$$

$$T'_s = \frac{L''_s}{R_s} = \frac{L_s}{R_s} - \frac{1}{R_s} \frac{j\omega_p L_m^2}{R_r + R_{ser} + j\omega_p L_r} \tag{19}$$

The variation of stator time constant with rotor braking resistor is shown in Figure 5. Comparing Equation (16) with Equation (19), it can be found that the rotor braking resistor enhances the real part of the stator time constant. The imaginary part of stator time constant has a maximum that can be ignored in the calculation. As a result, the transient stator flux linkage and the part of the rotor current that decrease with the stator time constant dampens slowly, which is harmful to the protection.

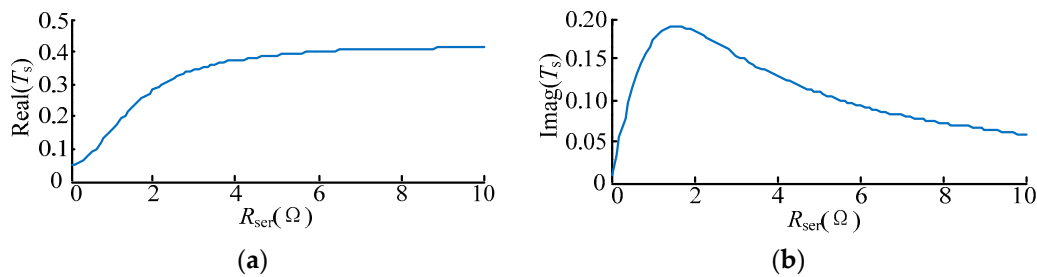


Figure 5. Equivalent circuit of the DFIG. (a) The real part of stator time constant; and (b) the imaginary part of stator time constant.

In this circumstance, to prevent the stator time constant becomes too large to affect the protection, the resistor should be optimized rather than fixed in different grid faults. As a result, a rotor braking resistor array is proposed in Figure 6. The equivalent resistance of the resistor array can be regulated through the switch. When a slight fault occurs, a low equivalent resistance is adopted so that the stator time constant cannot be enhanced too much.

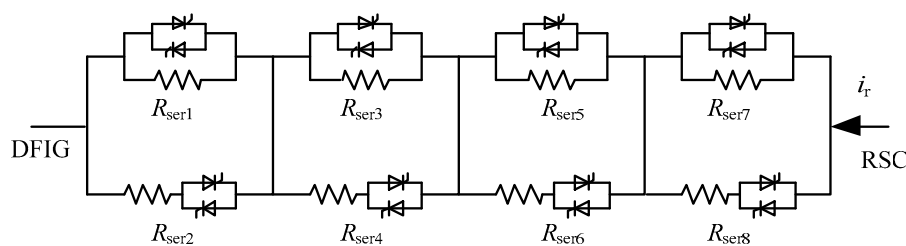


Figure 6. Rotor braking resistor array.

In order to further decrease the stator time constant and improves the damping speed, a crowbar circuit is proposed operating with the rotor braking circuit. The crowbar circuit is helpful to consume the excess energy in the rotor circuit and relieves the effect brought by the enhancement of the stator time constant. When the crowbar and the rotor braking resistor are operating together, the stator time constant becomes:

$$T'_s = \frac{L''_s}{R_s} = \frac{L_s}{R_s} - \frac{1}{R_s} \frac{j\omega_p L_m^2}{(R_r + R_{ser} // R_{cb}) + j\omega_p L_r} \tag{20}$$

where R_{cb} is the equivalent resistor of the crowbar circuit in the AC side. It can be found that the stator time constant in Equation (20) decreases due to the crowbar operation, which is helpful to the protection.

3.2. Rotor Current Calculation and Parameter Selection Principle

When the proposed protection operates, the rotor equivalent circuit of the DFIG in Figure 2 can be redrawn as shown in Figure 7.

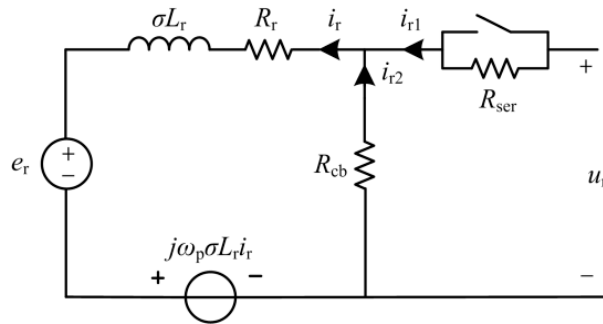


Figure 7. Rotor equivalent circuit of the DFIG.

The rotor current can be written as:

$$\begin{cases} 0 = e_r + \sigma L_r \frac{di_r}{dt} + j\omega_p \sigma L_r i_r + R_r i_r + R_{cb} i_{r2} \\ u_r = R_{ser} i_{r1} - R_{cb} i_{r2} \\ i_r = i_{r1} + i_{r2} \end{cases} \tag{21}$$

The control diagram of the RSC is shown in Figure 8 [23].

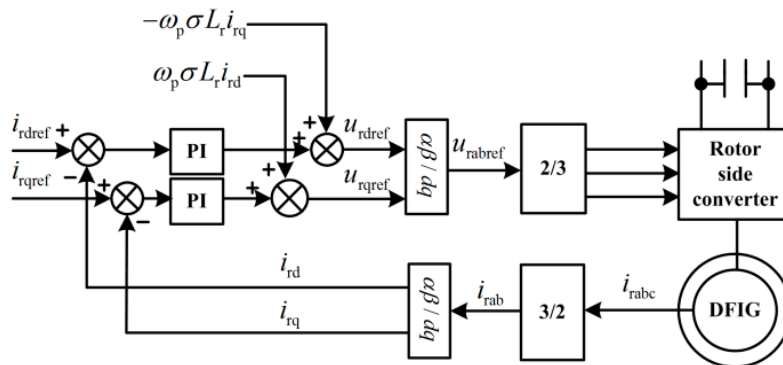


Figure 8. Rotor equivalent circuit of the DFIG.

The rotor voltage can be expressed as:

$$u_r = K_p(i_{r_ref} - i_r) + K_i \int (i_{r_ref} - i_r) dt + j\omega_p \sigma L_r i_r \tag{22}$$

where K_p and K_i are the parameters of the PI controller. i_{r_ref} is the reference of the rotor current. According to Equations (21) and (22), the differential equations are given:

$$\begin{cases} 0 = \frac{-R_{cb}}{R_{cb}+R_{ser}} \mathbf{u}_r + \mathbf{e}_r + \sigma L_r \frac{d\mathbf{i}_r}{dt} + (R_r + R_{cb} + j\omega_p \sigma L_r - \frac{R_{cb}^2}{R_{cb}+R_{ser}}) \mathbf{i}_r \\ \frac{du_r}{dt} = (R_{ser} + R_{cb}) \frac{di_{r1}}{dt} - R_{cb} \frac{di_r}{dt} \\ \frac{d\mathbf{u}_r}{dt} = (j\omega_p \sigma L_r - K_p) \frac{d\mathbf{i}_r}{dt} + K_i (\mathbf{i}_{r_ref} - \mathbf{i}_r) + j\omega_p \frac{L_m}{L_s} \frac{d\psi_s}{dt} \end{cases} \quad (23)$$

The analytical solution can be derived from Equations (7) and (23) and a parameter selection principle may be obtained. However, the analytical solution is a complex and long expression which makes it difficult to analyze the relation between the rotor current and the protection parameters. Compared with the analytical solution, the numerical solution is much simpler and has a clear expression. It is easy to obtain the curve that expresses the variation trend between the maximum rotor current and protection parameters, which provides a basis for protection parameter selection.

Taking a steady rotor current and the steady rotor voltage as the initial value of the numerical calculation, the rotor current and the RSC current is obtained through solving Equation (23). The calculation results are shown in Figures 9 and 10, which shows the variation of maximum transient rotor current under different protection parameters. With the increasing of R_{cb} and R_{ser} , rotor current in Figures 9a and 10a decreases obviously. This proves the effectiveness of the proposed protection. However, in Figures 9b and 10b, the RSC current increases with the increasing of R_{cb} . If a safety threshold of the rotor current is set, the protection parameters are determined in Figures 9 and 10.

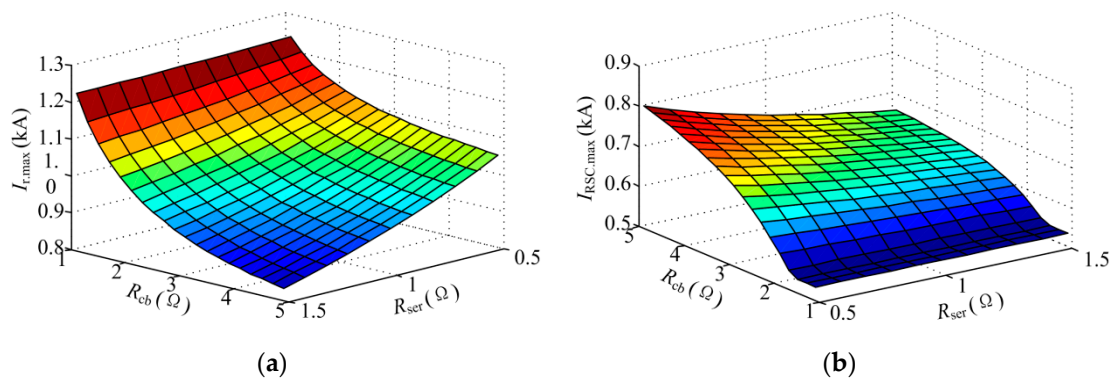


Figure 9. Calculation results under different parameters. (a) The maximum of the rotor current; and (b) the maximum of the RSC current.

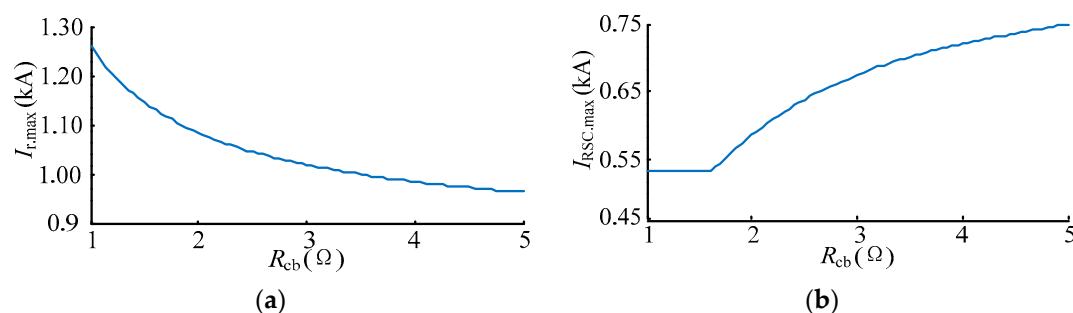


Figure 10. Calculation results under different crowbar resistors. (a) The maximum of the rotor current; and (b) the maximum of the RSC current.

During the fault time, the rotor current is divided into two parts: the crowbar current and the RSC current. The RSC current controls the active and reactive power that stator generates. However, the crowbar current forces a part of the DFIG to operate as an induction machine, which is likely to be the

conventional crowbar protection, and absorbs reactive power from the grid. Therefore, the parameter selection of the protection circuit ought to follow:

- (1) The R_{ser} and R_{cb} should be large enough to restrain the overcurrent and the R_{ser} cannot be quite as large, otherwise the control effect of the RSC would be poor due to the low RSC current.
- (2) The R_{cb} cannot be quite as large, otherwise the RSC current would exceed the safety threshold.
- (3) The R_{ser} ought to be less than R_{cb} . If R_{cb} is much less than R_{ser} , the DFIG almost operates as an induction machine. However, if R_{ser} is much less than R_{cb} , the RSC current may exceed the threshold value and the IGBTs are threatened to be damaged.

4. Corresponding Self-Adaptive Control Strategy

Normally, the rotor braking circuit protection circuit operates when the rotor current exceeds the safety threshold and quits operation when the rotor current is under the safety threshold. However, the rotor current may exceed the safety threshold repeatedly, which causes the repeating operation of the rotor braking circuit and cause electromagnetic impact on the DFIG.

To solve this issue, a self-adaptive control strategy is proposed, which controls the rotor braking circuit operating for the long-term. Moreover, to decrease the stator time constant and prevent the rotor current from being restrained excessively in the protection process, the equivalent resistance of the rotor braking resistor array would decrease gradually.

As a result, in the process of long-term protection, the value of protection resistance should be adjusted adaptively. The resistance that adopted should be obtained according to the maximum value of the RSC current after adjusting the resistance. Assuming that the resistance is adjusted at time t_{n1} , the stator transient flux linkage becomes:

$$\psi_{sn} = \frac{K_d U_{s0}}{j\omega_1} e^{-t_{n1}/T'_{s1}} e^{-j\omega_1 t} e^{-(t-t_{n1})/T'_{s2}} \quad (24)$$

where T'_{s1} is the stator time constant before adjustment and T'_{s2} is the stator time constant after adjustment. The stator transient flux linkage would dampen with T'_{s2} after t_{n1} . The rotor current, RSC current, and rotor voltage at t_{n1} can be measured, and then the RSC current is calculated through solving numerical solution of Equation (23). If the RSC current does not exceed the safety threshold, this resistance is adopted. If not, another resistance is given and the RSC current should be calculated once again.

For the proposed protection, the selection of protection exiting time is particularly important. If the protection exits too early, it would easily lead to the overcurrent again, and then the protection operates which causes unnecessary impact on the system.

If the protection exits late, it will affect the stability of the system and the control effect. Therefore, it is necessary to optimize and adjust the exiting time of protection during different faults. In order to obtain the optimal moment of protection resection, it is necessary to calculate the secondary overcurrent of the RSC after exiting. Assuming that the protection exits at the time t_x , the stator transient flux linkage becomes:

$$\psi_{sn} = \frac{(1 - K_d) U_{s0}}{j\omega_1} + \frac{K_d U_{s0}}{j\omega_1} e^{-T_x} e^{-j\omega_1 t} e^{-(t-t_x)/T_s} \quad (25)$$

where T_x is defined as the transient damping coefficient:

$$T_x = \frac{t_{n1}}{T'_{s1}} + \frac{t_{n2} - t_{n1}}{T'_{s2}} + \dots + \frac{t_{ni} - t_{n(i-1)}}{T'_{si}}, (i = 1, 2, \dots) \quad (26)$$

where T'_{si} ($i = 1, 2, \dots$) is the stator time constant in the process of the protection resistance variation. Measuring the rotor current, RSC current, and rotor voltage at t_x , the RSC current can be calculated through solving the differential equation in Equation (23).

The flow diagrams of self-adaptive control and calculation are illustrated in Figure 11. The proposed control consists of the following four parts:

- (1) Protection operation: When the fault of external power grid causes voltage sag, it will cause the rotor overcurrent of the DFIG. The protection would operate at the time that a rotor overcurrent exceeds the action value.
- (2) Calculation of resistance: The resistance should be calculated before protection operation according to voltage sag depth, rotor current, and voltage.
- (3) Adaptive adjustment of rotor braking resistance: The long-term protection and adaptive adjustment of resistance value is adopted. During the protection process, the protection resistance decreases once in a power frequency cycle.
- (4) Protection exiting: Assuming that the protection exits at the current moment, the RSC overcurrent after the exiting is calculated according to the calculation flow. If the calculation result meets the safety threshold, the protection can exit at this moment.

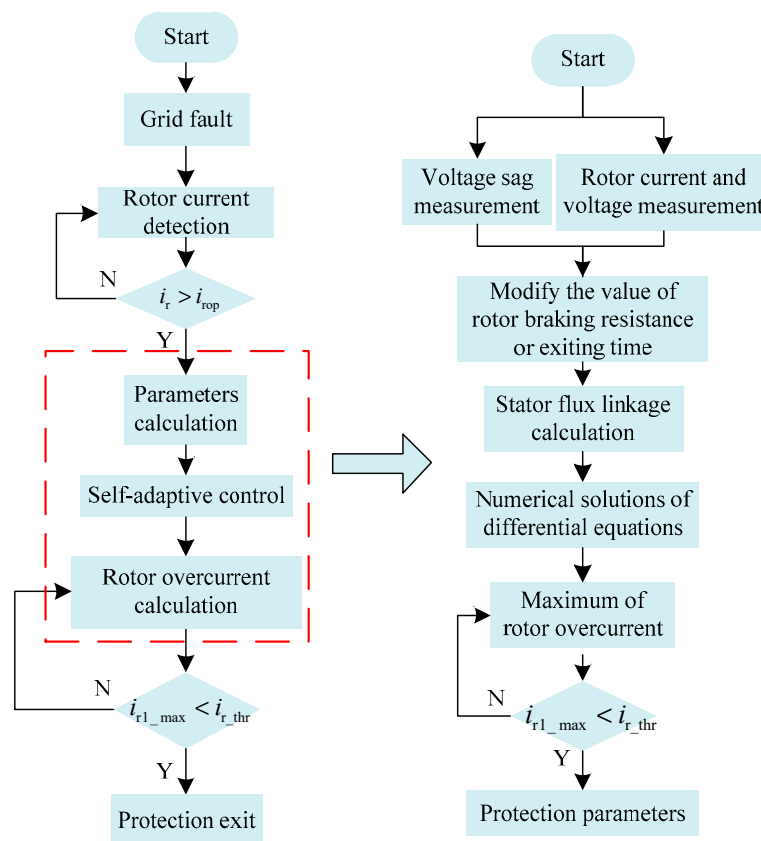


Figure 11. Flow diagram of the self-adaptive control.

5. Proposed Protection Performance

To verify the effectiveness of the proposed protection circuit and corresponding control strategy, a 1.5 MW DFIG simulation model is employed in Figure 12. The wind speed is maintained at 13m/s and the slip rate is -0.2 . A symmetrical voltage dip at grid occurs at 2 s and continues for 0.5 s.

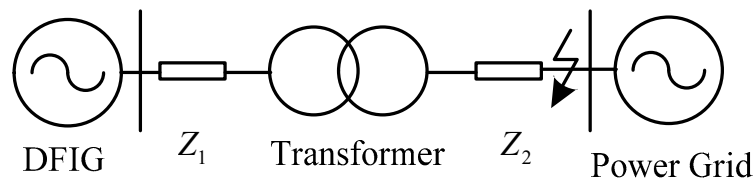


Figure 12. Simulation model of the DFIG.

The parameters of the DFIG, transformer, and power grid are shown in Table 1:

Table 1. Parameters of the simulation model.

DFIG rated capacity	1.5 MW	Line voltage	690 V	Rated speed	1500 r/min
Stator resistance	0.023 pu	Rotor resistance	0.016 pu	Stator leakage inductance	0.18 pu
Rotor leakage inductance	0.16 pu	Magnetic inductance	2.9 pu	Ratio of stator and rotor	0.35
Transformer capacity	1.6 MW	Transformer ratio	0.69/35	Leakage reactance	6.5%
Grid voltage	35 kV	Line length	7 km	Impedance of line	$0.3 + j0.4 \Omega/\text{km}$

The comparisons of the RSC current under different voltage sags between simulation and calculation are shown in Figure 13. Ignoring the impedance of the transformer and line, the calculation results are the numerical solution of the rotor current gained according to the rotor current calculation method shown in Sections 3 and 4. The simulation results are gained in simulation platform according to the simulation model. It can be found that the variation tendency and value of the calculated results are close to the simulation results. When the protection exits, the calculated RSC overcurrent is also similar to that in the simulation. As a result, the calculation method introduced in Figure 11 can be used in the self-adaptive control and the parameters of protection can be optimized.

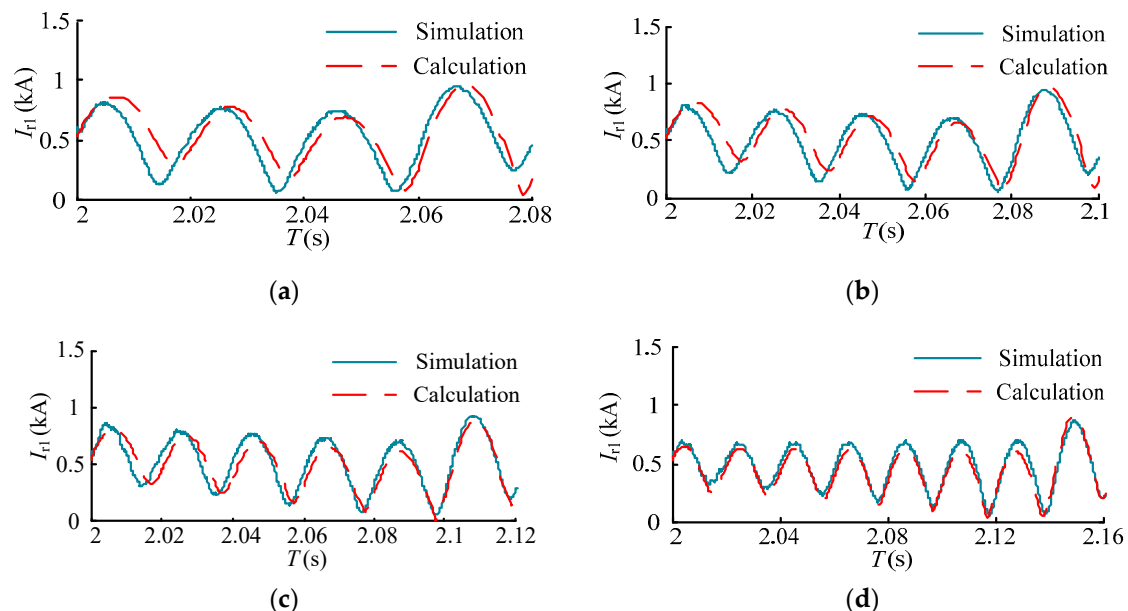


Figure 13. Comparison between calculation and simulation. (a) Voltage sag of 0.5; (b) voltage sag of 0.6; (c) voltage sag of 0.7; and (d) voltage sag of 0.8.

The performances of the proposed protection with the corresponding self-adaptive control strategy under different voltage sags are shown in Figures 14 and 15. The transient responses without any protection are also shown. The resistance of rotor braking circuit changes gradually every 0.2 s and the protection exits at 2.08 s and 2.14 s. The DC-link overvoltage and rotor overcurrent are surely threatening the security of DC-link bus and RSC without any protection. In the proposed protection, the overcurrent and overvoltage are restrained effectively. The impact of electromagnetic torque is also restrained. Moreover, the RSC avoids being blocked and the value of the RSC current is below 0.8 kA, which guarantees the IGBTs are not be damaged and the RSC operates normally. The ripples of the RSC current and rotor current are also restrained with the proposed protection.

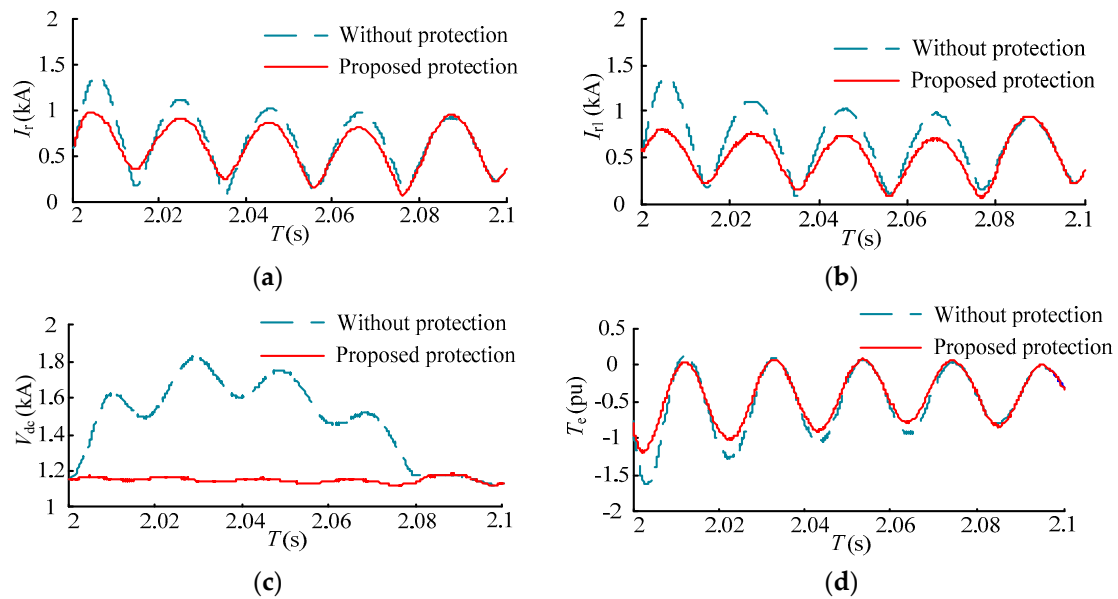


Figure 14. Response of proposed protection under a voltage sag of 0.6. (a) Rotor current; (b) RSC current; (c) DC-link bus voltage; and (d) electromagnetic torque.

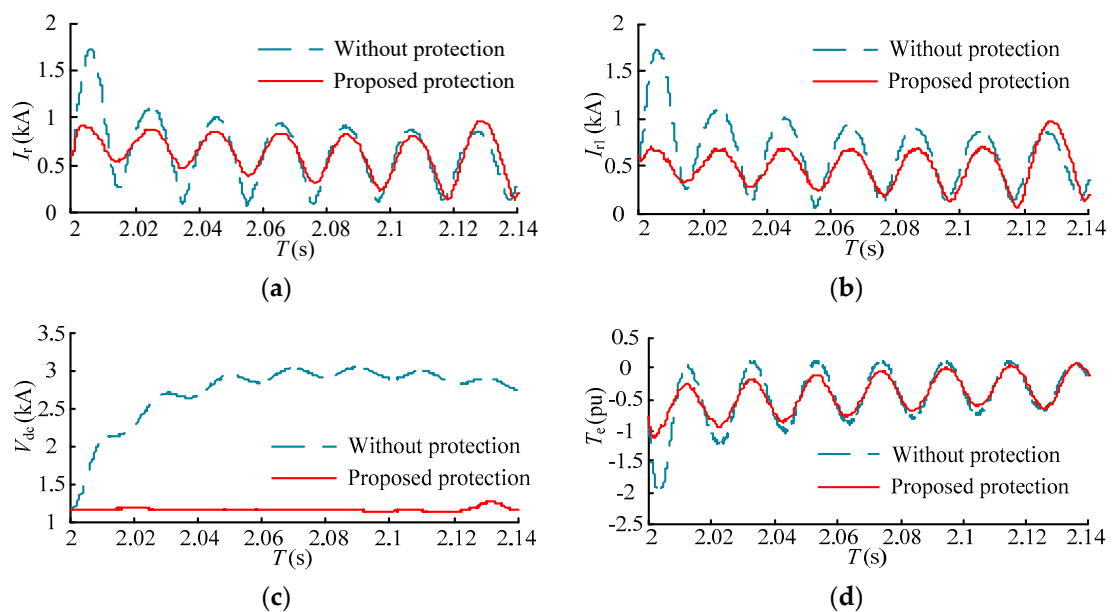


Figure 15. Response of proposed protection under a voltage sag of 0.8. (a) Rotor current; (b) RSC current (c) DC-link bus voltage; and (d) electromagnetic torque.

The comparisons between proposed protection and conventional crowbar protection are shown in Figures 16 and 17. Although the conventional crowbar protection restrains the rotor current, DC-link bus voltage, and electromagnetic torque effectively, the PWM signals of the RSC are locked to protect the IGBT. As a result, the DFIG loses the reactive power control ability and operates as a induction motor, which may consume reactive power and deepen the voltage sag.

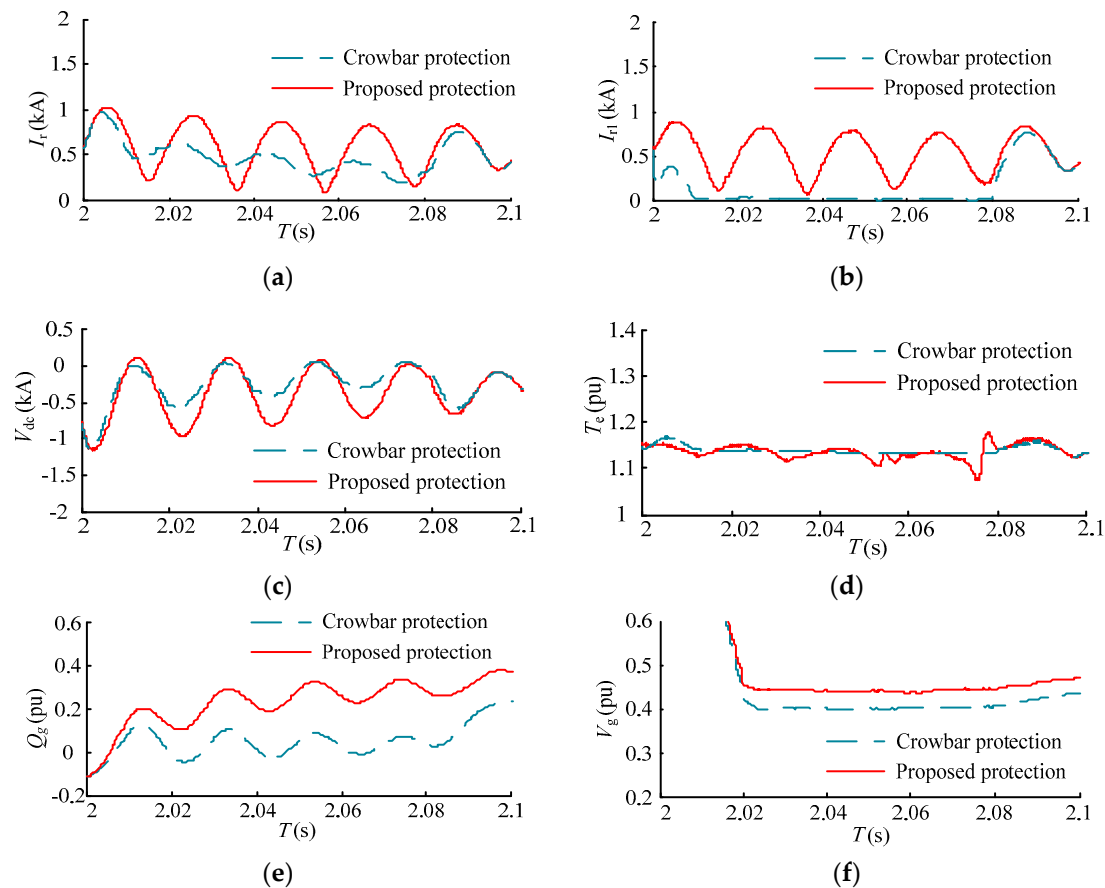


Figure 16. Comparisons between proposed protection and crowbar protection under a voltage sag of 0.6. (a) Rotor current; (b) RSC current; (c) electromagnetic torque; (d) DC-link bus voltage; (e) reactive power at the grid; and (f) the terminal voltage.

When the proposed protection is adopted, the rotor overcurrent and DC-link bus overvoltage are also avoided. Moreover, the reactive power control ability of the DFIG is retained during the protection operation. As a result, the rotor current is larger than that under crowbar protection. In Figure 16e,f below, the DFIG generates 0.3 pu of reactive power to the grid and the terminal voltage is enhanced 0.05 pu. This cannot be ignored if each DFIG of a large-scale wind farm generates reactive power.

In [7], the rotor braking resistor and chopper protection are adopted for the LVRT. The operation of the protection is controlled by a safety threshold. The protection operates at the moment that the rotor current or the DC-link bus voltage exceeds the safety threshold and exits at the moment that the rotor current or the DC-link bus voltage is under the safety threshold. The comparisons between protection in [7] and the proposed protection in this paper are shown in Figures 18 and 19.

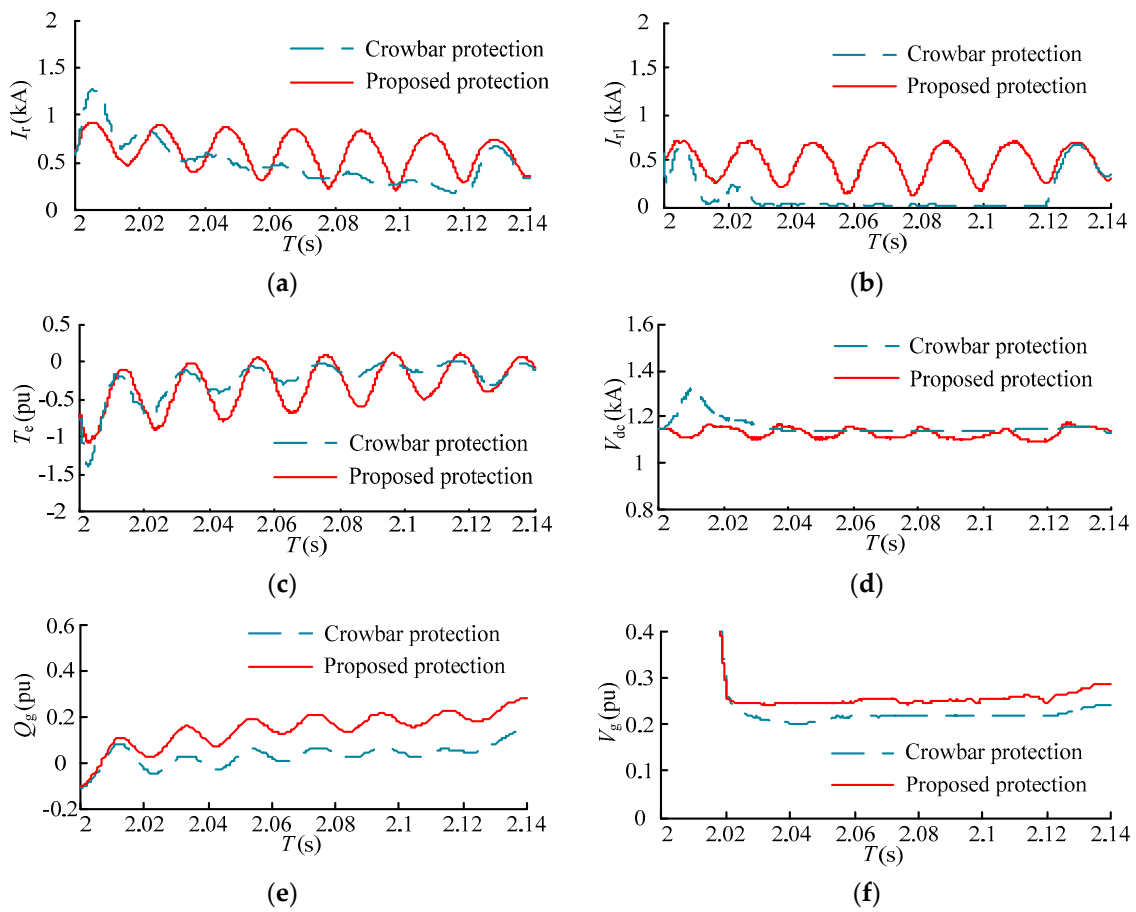


Figure 17. Comparisons between proposed protection and crowbar protection under a voltage sag of 0.8. (a) Rotor current; (b) RSC current; (c) electromagnetic torque; (d) DC-link bus voltage; (e) reactive power at the grid; and (f) the terminal voltage.

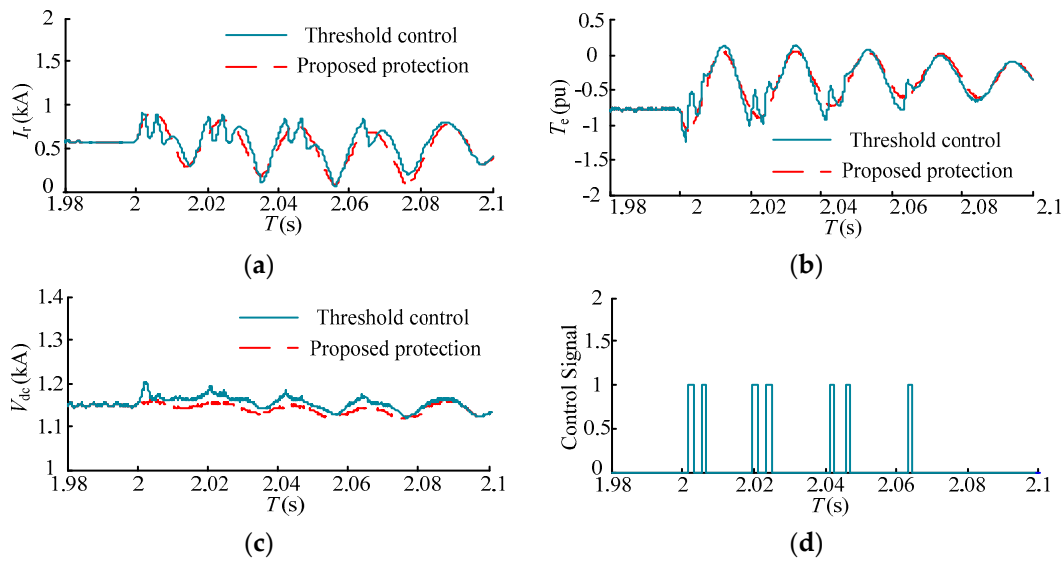


Figure 18. Comparisons between proposed protection and threshold control under a voltage sag of 0.6. (a) Rotor current; (b) electromagnetic torque; (c) DC-link bus voltage; and (d) the control signal of rotor braking resistor.

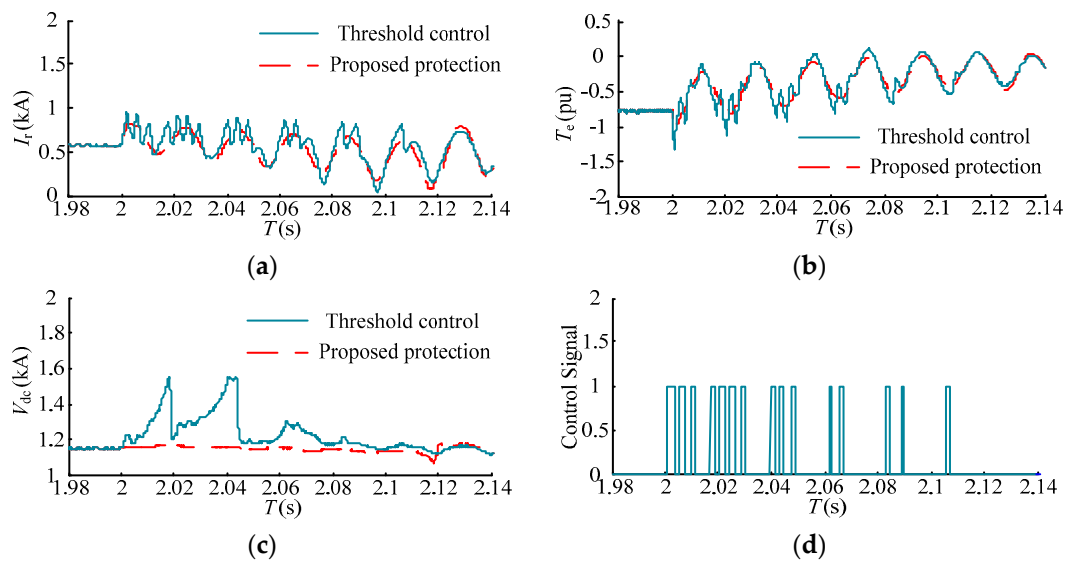


Figure 19. Comparisons between proposed protection and threshold control under a voltage sag of 0.8. (a) Rotor current; (b) electromagnetic torque; (c) DC-link bus voltage; and (d) the control signal of rotor braking resistor.

From Figures 18d and 19d, the protection operates and exits repeatedly during the fault period, which causes several impacts of the rotor current and electromagnetic torque. Additionally, the DC-link bus voltage reaches the operating value of the chopper protection and the chopper protection operates under a voltage sag of 0.8. However, the proposed protection operates for the long-term and ensures the rotor current is smooth. As a result, several impacts are avoided. Moreover, the DC-link bus voltage is retained around the steady-state value under the proposed protection, which does not need the coordination of chopper protection.

The comparison of the performance between proposed protection and the fixed rotor braking resistor is shown in Figure 20. A fixed resistor can restrain the rotor overcurrent, DC-link bus overvoltage, and the impact of electromagnetic torque more effectively. However, the RSC current is restrained excessively under a fixed resistor and, hence, the reactive power is lower than that under the proposed method. The stator transient flux linkage damps slowly due to the fixed resistor. As a result, the rotor current exceeds the safety threshold and the DC-link bus voltage is enhanced after the fixed rotor braking resistor, exiting at 2.08 s. The proposed protection controls the switch of the resistor array and the equivalent resistance decreases gradually, which ensures that the rotor current is maintained at the appropriate value and the stator transient flux linkage damps quickly. Moreover, the crowbar also decreases the stator time constant and further accelerates the damping of the stator time constant. Therefore, the rotor current cannot exceed the safety threshold after 2.08 s.

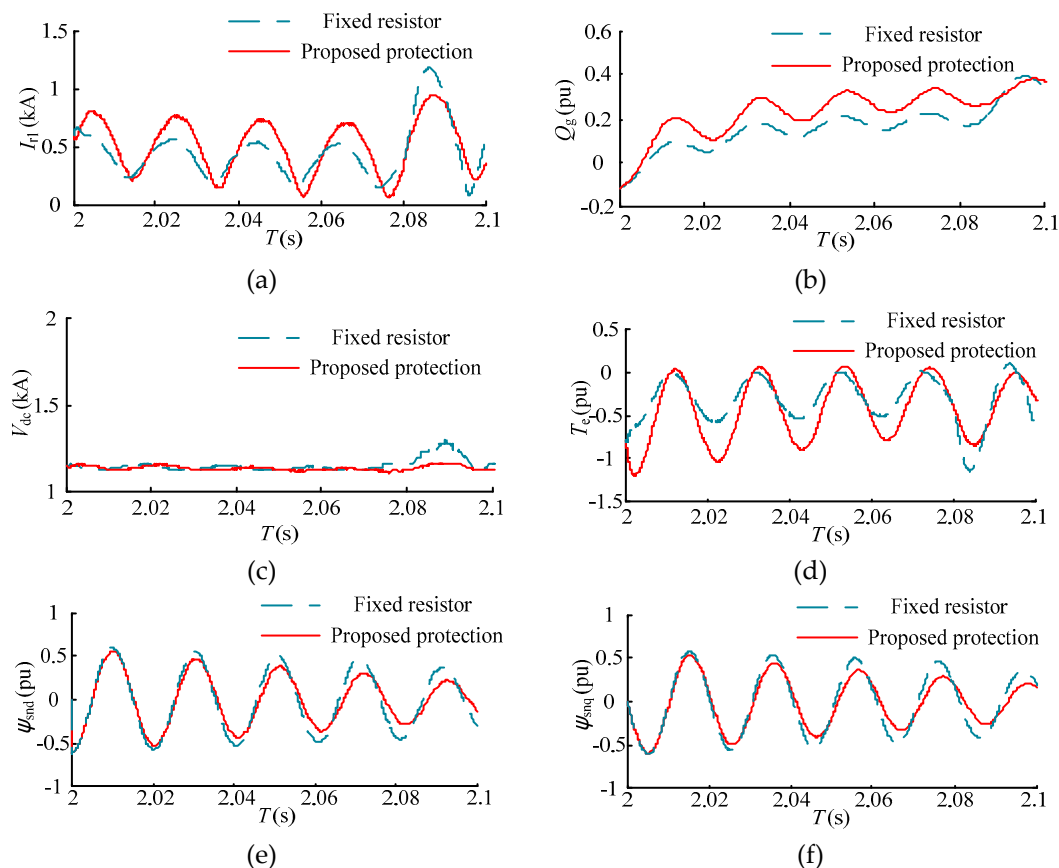


Figure 20. Comparison between proposed protection and fixed rotor braking resistor. (a) RSC current; (b) reactive power at the grid; (c) DC-link bus voltage; (d) electromagnetic torque; (e) the D-axis component of the stator transient flux linkage; and (f) the Q-axis component of the stator transient flux linkage.

6. Conclusion

In order to enhance the LVRT ability of the DFIG, an improved rotor braking circuit is adopted in this work. The rotor equivalent circuit of the DFIG and the differential equations are presented and, hence, a selection principle for the protection parameters is illustrated. To adapt the proposed protection, a self-adaptive control is presented, which regulates the resistance and exiting time of the protection and relieves the effect that brought by rotor braking circuit during the grid fault.

The rotor overcurrent is restrained through the proposed protection, and the ripples of rotor current and DC-link voltage are also reduced. Although the fluctuation of rotor current and the electromagnetic torque under the proposed protection is slightly larger in comparison with conventional crowbar protection, the fluctuation can be accepted and the proposed protection avoids blocking the RSC and retains reactive power control ability during the grid fault. According to the parameter selection, the RSC current and rotor current remains at an appropriate value. The enhancement of the stator time constant by the rotor braking resistor is relieved and the damping of the stator transient flux linkage is accelerated through a self-adaptive control strategy. Compared with the fixed rotor braking resistor, the reactive power ability is enhanced. Moreover, the rotor secondary overcurrent and repeated operation can be avoided by a long-term protection and the calculation of the exiting time. Hence, several impacts of rotor current and electromagnetic torque are relieved.

Author Contributions: All of the authors contributed to this work. J.C. put forward the idea and gave guidance; Y.W. performed the modeling and simulation and wrote the manuscript; M.Z. provided professional advice and reviewed the paper; Q.Y. and J.L. processed the simulation data.

Funding: This research received no external funding.

Conflicts of Interest: The authors declare no conflict of interest.

References

1. Ackermann, T. *Wind Power in Power Systems*; John Wiley: Chichester, UK; Hoboken, NJ, USA, 2005.
2. Abdel-Baqi, O.; Nasiri, A. A dynamic LVRT solution for Doubly-Fed Induction Generator. In Proceedings of the 2009 35th Annual Conference of IEEE Industrial Electronics, Porto, Portugal, 3–5 November 2009; pp. 825–830.
3. Yang, L.; Xu, Z.; Ostergaard, J.; Dong, Z.Y.; Wong, K.P. Advanced Control Strategy of the DFIG Wind Turbines for Power System Fault Ride Through. *IEEE Trans. Power Syst.* **2012**, *27*, 713–722. [[CrossRef](#)]
4. Pannell, G.; Atkinson, D.J.; Zahawi, B. Minimum-Threshold Crowbar for a Fault-Ride-Through Grid-Code-Compliant DFIG Wind Turbine. *IEEE Trans. Energy Convers.* **2010**, *25*, 750–759. [[CrossRef](#)]
5. Huchel, L.; Moursi, M.S.E.; Zeineldin, H.H. A Parallel Capacitor Control Strategy for Enhanced FRT Capability of the DFIG. *IEEE Trans. Sustain. Energy* **2015**, *6*, 303–312. [[CrossRef](#)]
6. Swain, S.; Ray, P.K. Short circuit fault analysis in a grid connected DFIG based wind energy system with active crowbar protection circuit for ridethrough capability and power quality improvement. *Int. J. Electr. Power Energy Syst.* **2017**, *84*, 64–75. [[CrossRef](#)]
7. Yang, J.; Fletcher, J.E.; O'Reilly, J. A Series-Dynamic-Resistor-Based Converter Protection Scheme for Doubly-Fed Induction Generator During Various Fault Conditions. *IEEE Trans. Energy Convers.* **2010**, *25*, 422–432. [[CrossRef](#)]
8. Causebrook, A.; Atkinson, D.J.; Jack, A.G. Fault Ride-Through of Large Wind Farms Using Series Dynamic Braking Resistors. *IEEE Trans. Power Syst.* **2007**, *22*, 966–975. [[CrossRef](#)]
9. Mohammadi, J.; Afsharnia, S.; Vaez-Zadeh, S.; Farhangi, S. Improved fault ride through strategy for doubly fed induction generator based wind turbines under both symmetrical and asymmetrical grid faults. *IET Renew. Power Gener.* **2016**, *10*, 1114–1122. [[CrossRef](#)]
10. El-helw, H.; Khaled, A. Comparison study between two Dynamic Breaking resistor techniques in protecting the doubly fed induction generator. In Proceedings of the 2013 12th International Conference on Environment and Electrical Engineering, Wroclaw, Poland, 5–8 May 2013; pp. 25–29.
11. Wessels, C.; Gebhardt, F.; Fuchs, F.W. Fault Ride-Through of a DFIG Wind Turbine Using a Dynamic Voltage Restorer During Symmetrical and Asymmetrical Grid Faults. *IEEE Trans. Power Electron.* **2011**, *26*, 807–815. [[CrossRef](#)]
12. Justo, J.J.; Bansal, R.C. Parallel R-L configuration crowbar with series R-L circuit protection for LVRT strategy of the DFIG under transient-state. *Electr. Power Syst. Res.* **2018**, *154*, 299–310. [[CrossRef](#)]
13. Justo, J.J.; Mwasilu, F.; Jung, J.-W. Enhanced crowbarless FRT strategy for DFIG based wind turbines under three-phase voltage dip. *Electr. Power Syst. Res.* **2017**, *142*, 215–226. [[CrossRef](#)]
14. Zheng, Z.; Huang, C.; Yang, R.; Xiao, X.; Li, C. A Low Voltage Ride Through Scheme for DFIG-Based Wind Farm with SFCL and RSC Control. *IEEE Trans. Appl. Supercond.* **2019**, *29*, 1–5. [[CrossRef](#)]
15. Du, K.; Xiao, X.; Wang, Y.; Zheng, Z.; Li, C. Enhancing Fault Ride-Through Capability of the DFIG-Based Wind Turbines Using Inductive SFCL With Coordinated Control. *IEEE Trans. Appl. Supercond.* **2019**, *29*. [[CrossRef](#)]
16. Zou, Z.; Liao, J.; Lei, Y.; Mu, Z.; Xiao, X. Postfault LVRT Performance Enhancement of the DFIG Using a Stage-Controlled SSFCL-RSDR. *IEEE Trans. Appl. Supercond.* **2019**, *29*. [[CrossRef](#)]
17. Firouzi, M.; Gharehpetian, G.B. LVRT Performance Enhancement of the DFIG-Based Wind Farms by Capacitive Bridge-Type Fault Current Limiter. *IEEE Trans. Sustain. Energy* **2018**, *9*, 1118–1125. [[CrossRef](#)]
18. Chang, Y.; Kong, X. Linear demagnetizing strategy of the DFIG-based WTs for improving LVRT responses. *J. Eng.* **2017**, *13*, 2287–2291. [[CrossRef](#)]
19. Wang, M.; Shi, Y.; Zhang, Z.; Shen, M.; Lu, Y. Synchronous Flux Weakening Control with Flux Linkage Prediction for Doubly-Fed Wind Power Generation Systems. *IEEE Access* **2017**, *5*, 5463–5470. [[CrossRef](#)]
20. Zhu, D.; Zou, X.; Deng, L.; Huang, Q.; Zhou, S.; Kang, Y. Inductance-Emulating Control for DFIG-Based Wind Turbine to Ride-Through Grid Faults. *IEEE Trans. Power Electron.* **2017**, *32*, 8514–8525. [[CrossRef](#)]
21. Baiju, P.; Rajeev, T. Low Voltage Ride Through in DFIG based wind turbines: A review. In Proceedings of the 2015 International Conference on Control Communication Computing India (ICCC), Trivandrum, India, 19–21 November 2015; pp. 337–342.

22. Kauffmann, T.; Karaagac, U.; Kocar, I.; Jensen, S.; Mahseredjian, J.; Farantatos, E. An Accurate Type III Wind Turbine Generator Short Circuit Model for Protection Applications. *IEEE Trans. Power Deliv.* **2017**, *32*, 2370–2379. [[CrossRef](#)]
23. Xiong, X.; Ouyang, J. Analysis and calculation of rotor currents for doubly-fed induction generators under short circuits in power grids. *Proc. CSEE* **2012**, *32*, 114–121.



© 2019 by the authors. Licensee MDPI, Basel, Switzerland. This article is an open access article distributed under the terms and conditions of the Creative Commons Attribution (CC BY) license (<http://creativecommons.org/licenses/by/4.0/>).